

# Observation of the simplest Criegee intermediate CH<sub>2</sub>OO in the gas-phase ozonolysis of ethylene

Caroline C. Womack,<sup>1</sup> Marie-Aline Martin-Drumel,<sup>2</sup> Gordon G. Brown,<sup>3</sup>  
Robert W. Field,<sup>1</sup> Michael C. McCarthy<sup>2\*</sup>

2015 © The Authors, some rights reserved;  
exclusive licensee American Association for  
the Advancement of Science. Distributed  
under a Creative Commons Attribution  
Non-Commercial License 4.0 (CC BY-NC).  
10.1126/sciadv.1400105

Ozonolysis is one of the dominant oxidation pathways for tropospheric alkenes. Although numerous studies have confirmed a 1,3-cycloaddition mechanism that generates a Criegee intermediate (CI) with form R<sub>1</sub>R<sub>2</sub>COO, no small CIs have ever been directly observed in the ozonolysis of alkenes because of their high reactivity. We present the first experimental detection of CH<sub>2</sub>OO in the gas-phase ozonolysis of ethylene, using Fourier transform microwave spectroscopy and a modified pulsed nozzle, which combines high reactant concentrations with rapid sampling and sensitive detection. Nine other product species of the O<sub>3</sub> + C<sub>2</sub>H<sub>4</sub> reaction were also detected, including formaldehyde, formic acid, dioxirane, and ethylene ozonide. The presence of all these species can be attributed to the unimolecular and bimolecular reactions of CH<sub>2</sub>OO, and their abundances are in qualitative agreement with published mechanisms and rate constants.

## INTRODUCTION

Ozonolysis is one of the most common oxidation pathways for unsaturated hydrocarbons in the troposphere. It is the predominant sink for biogenic and anthropogenic alkenes and is a significant source of OH radicals (1), but many aspects of this complex reaction pathway remain poorly understood even after decades of study (1–4). It is generally understood, however, that the reaction proceeds via a concerted 1,3-cycloaddition of O<sub>3</sub> across the alkene double bond, through a van der Waals complex, to form a 1,2,3-trioxolane primary ozonide (denoted as a POZ, and shown in Fig. 1). This initial step is highly exothermic; consequently, the POZ is formed with high vibrational energy and promptly decomposes to form a carbonyl and a carbonyl oxide, which is commonly referred to as a Criegee intermediate (CI) (2). Although a portion of the internal energy in the POZ is lost to translational and rotational degrees of freedom of the two fragments, the CI is formed with a considerable amount of vibrational energy (5).

Nascent CIs are generally categorized as either “excited” CIs, which have sufficient vibrational energy to isomerize or dissociate rapidly, or “stabilized” CIs (SCIs), which had been initially formed with high vibrational energy but have been stabilized by collisional energy transfer. However, SCIs remain quite reactive owing to their zwitterionic character (6, 7) and undergo rapid bimolecular reaction with other atmospheric species; as such, only one instance of a SCI resulting from gas-phase ozonolysis has been reported, albeit at low resolution (8). Theoretical and indirect experimental studies (9) have determined the branching fraction to SCI to be as high as 0.54 for CH<sub>2</sub>OO formed in the ozonolysis of ethylene (10). The branching fraction for larger SCIs is highly dependent on a number of factors, including temperature, pressure, and the nature of its substituents (11). A schematic of the initial reaction pathways for the ozonolysis of ethylene, the simplest alkene, is shown in Fig. 1.

Although the Criegee mechanism is now widely accepted (12), CIs eluded direct detection in the gas phase until 2008, when Taatjes *et al.* (13) measured the simplest CI, CH<sub>2</sub>OO (2), by photolysis of dimethyl sulfoxide and photoionization mass spectroscopy. In 2012, the same

group showed that the photolysis of diiodomethane (CH<sub>2</sub>I<sub>2</sub>) in the presence of excess molecular oxygen was a more efficient method for selectively generating CH<sub>2</sub>OO (14). This production method has since been used by many groups to measure the vibrational (15), rotational (16–18), and electronic (19, 20) spectra of small CIs, as well as to study their reactivity with common atmospheric molecules (7, 8, 21–23). Although this method has been enormously valuable in characterizing the spectroscopy and kinetics of CH<sub>2</sub>OO, a number of questions remain about the product branching of the nascent CIs formed directly from ozonolysis. Furthermore, the generation of larger CIs with the photolysis method is contingent on the availability of analogously larger diiodo-substituted precursors. For these reasons, we have studied the ozonolysis of ethylene at atmospheric pressure and temperature, using Fourier transform microwave (FTMW) spectroscopy and a modified pulsed nozzle. This work has resulted in the detection of species ranging from the pre-reactive complex to secondary reaction products. Most significantly, the simplest CI, CH<sub>2</sub>OO, was detected in trace amounts.

## RESULTS AND DISCUSSION

The first step of the O<sub>3</sub> + C<sub>2</sub>H<sub>4</sub> reaction is highly exothermic ( $\Delta H \approx -50$  kcal/mol) (24, 25), but the overall reaction rate coefficient is relatively small ( $1.45 \times 10^{-18}$  cm<sup>3</sup> molecule<sup>-1</sup> s<sup>-1</sup>) (10). Nascent CH<sub>2</sub>OO is highly reactive with many species, including the O<sub>3</sub> and C<sub>2</sub>H<sub>4</sub> reactants. For these reasons, detection of CH<sub>2</sub>OO likely requires (i) large concentrations of O<sub>3</sub> and C<sub>2</sub>H<sub>4</sub> to ensure a high reaction rate, (ii) rapid sampling after the two reactants are mixed to minimize secondary chemistry, and (iii) an exquisitely sensitive and selective detection method capable of measuring many different species at parts per billion concentrations (that is,  $\sim 10^9$  molecules/pulse). The Balle-Flygare type cavity FTMW spectrometer used in these experiments (16, 26), described in Materials and Methods fulfills this last requirement. To address the second requirement, we constructed a nozzle source (see Fig. 2) based on the design of Lovas *et al.* (27, 28), who studied the O<sub>3</sub>···C<sub>2</sub>H<sub>4</sub> complex by “freezing” the products mid-reaction through supersonic expansion into a vacuum chamber.

In total, nine product species were detected in our experiment at room temperature and pressure. All required the presence of both O<sub>3</sub> and

<sup>1</sup>Department of Chemistry, Massachusetts Institute of Technology, Cambridge, MA 02139, USA. <sup>2</sup>Harvard-Smithsonian Center for Astrophysics, Cambridge, MA 02138, USA. <sup>3</sup>Department of Science and Mathematics, Coker College, Hartsville, SC 29550, USA.  
\*Corresponding author. E-mail: mmccarthy@cfa.harvard.edu

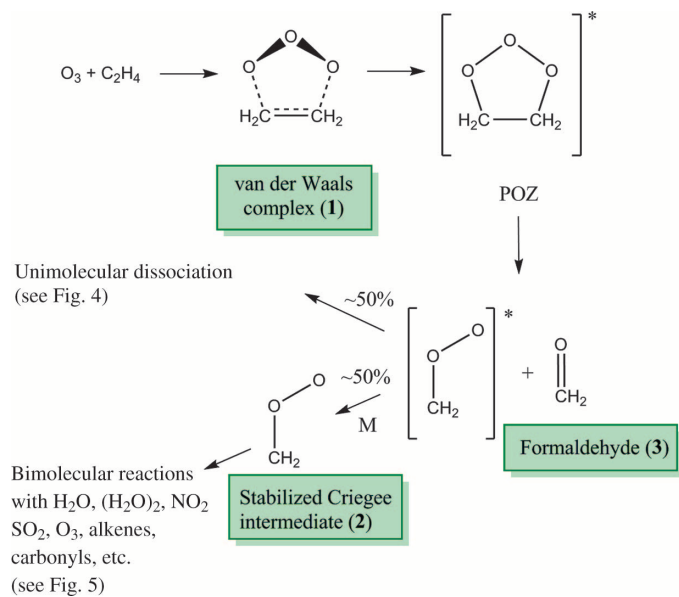


**Fig. 1. The initial reactions in the ozonolysis of ethylene.** The reaction proceeds through a van der Waals complex and then forms a high-energy primary ozonide, which immediately decomposes into a Cl and formaldehyde. Depending on the energy available, the Cl may undergo unimolecular dissociation or bimolecular reactions with other atmospheric species. Shaded text boxes indicate species detected in our experiment.

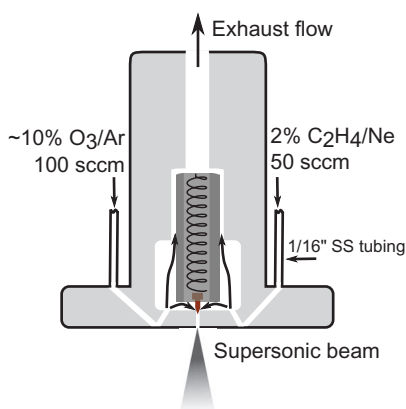


**Fig. 2. A schematic of a fast-flow reactor to rapidly sample products of the  $O_3 + C_2H_4$  reaction.** The reactants were passed through 1/16-inch inlets into the inner body of the nozzle. The armature, poppet, and spring in the center of the nozzle controlled the flow of 3.5% of the reacting mixture into the detector, while the remainder of the sample was exhausted to a fume hood. Further details may be found in Materials and Methods.

$C_2H_4$  and were sensitive to the flow rates and relative  $O_3$  and  $C_2H_4$  concentrations. The signal attributed to  $CH_2OO$ , shown in Fig. 3, was scrutinized carefully. Although weak, the frequency of this line matches the published high-resolution data (16, 17) to within 3 kHz, and we ensured that it was not an oscilloscope artifact or image by shifting the probe frequency. Additionally, the line vanished when a second microwave source, aligned perpendicularly to the cavity axis in a double resonance scheme, excited the  $2_{0,2}-1_{0,1}$  transition (16, 17). For these reasons, the line can be unequivocally attributed to  $CH_2OO$ . Its

signal intensity corresponds to about  $5.9 \times 10^9$  molecules/pulse, which is close to the detection limit of the microwave spectrometer. Other detected species are listed in Table 1. All can be attributed to established secondary chemistry of the  $O_3 + C_2H_4$  reaction, as illustrated in Figs. 4 and 5, and discussed below. A small number of the product species in the figures were not detected, because they either could not be detected in our spectrometer, were too reactive, or do not have published rotational lines.

Figure 4 illustrates the two unimolecular pathways available for excited  $CH_2OO$ , denoted as the “hot ester” and “hydrogen transfer” mechanisms. The hot ester pathway involves a ring-closing mechanism to form dioxirane (4), then O-O bond cleavage through an unstable dioxymethylene intermediate (5) to make formic acid (6). This pathway was experimentally verified by the matrix isolation FTIR experiments of Lovas *et al.* (32), and we detected dioxirane and formic acid in high relative concentrations: 50 and 3300 times that of  $CH_2OO$ , respectively. Dioxymethylene is very reactive and has not been studied in the microwave region and, consequently, was not measured here. Some fraction of formic acid was presumably formed with sufficient vibrational energy to isomerize to  $CO_2 + H_2$  and  $CO + H_2O$ , but these two- and three-atom species do not have rotational frequencies in the 5 to 42 GHz range of our spectrometer. There is also some evidence of  $HCO + OH$  formation (38), but  $HCO$  cannot be measured in our spectrometer, and  $OH$  was not observed, likely because of its reactivity.

The second pathway available is the hydrogen transfer mechanism. In Cls with hydrocarbon substituents in the *syn* position, this pathway is a 1,4-hydrogen transfer and is highly favored, leading to either stabilized vinyl hydroperoxides or OH radicals (1, 3, 5). Indeed, this pathway is thought to be the dominant source of nighttime hydroxyl radicals in the troposphere (4). Because of the absence of  $\beta$ -hydrogens,  $CH_2OO$  may instead undergo a 1,3-hydrogen transfer to the unstable hydroperoxymethylene (7), which immediately decomposes to  $HCO + OH$ . The microwave spectrum of 7 has not been previously measured and was therefore not measured here. However, this pathway is believed to have a barrier height more than 13 kcal/mol higher than the hot ester pathway (39) and is thus expected to be a minor reaction.

Figure 5 shows the major bimolecular reaction pathways of  $CH_2OO$  in our experiment. Under true atmospheric conditions, the reaction of  $CH_2OO$  with water is believed to be its dominant pathway (1) because of the prevalence of water in the troposphere (40). Other key co-reactants include  $SO_2$ ,  $NO_2$ , and the water dimer; the reactivity of  $CH_2OO$  with each has been well studied (23, 40–42). Reactions with ozone, alkenes, and carbonyl oxides have also been studied (43), but are less important in the atmosphere because of the relative scarcity of these molecules. Under our experimental conditions, however,  $O_3$ ,  $C_2H_4$ , and  $CH_2O$  are present in high abundance, and thus, the bimolecular chemistry with  $CH_2OO$  is dominated by the reactions of these three species.

$CH_2OO$  is highly reactive with carbonyl groups, and formaldehyde (3) is the most prevalent carbonyl in our system, not only because it is the cofragment of POZ decomposition but also because many bimolecular reactions of  $CH_2OO$  yield formaldehyde. Indeed, Table 1 shows that formaldehyde is present in concentrations three orders of magnitude greater than any other product. The reaction with formaldehyde (reaction A; Fig. 5) proceeds through ethylene ozonide (8, also called 1,2,4-trioxolane or the secondary ozonide), which immediately decomposes to hydroxymethyl formate (9) or formaldehyde and formic acid.

**Table 1. Products species detected in the O<sub>3</sub> + C<sub>2</sub>H<sub>4</sub> reaction.** Bold parenthetical numbers refer to species in Figs. 4 and 5. Rotational transitions of each product were monitored at the frequencies listed in the third column, which are obtained from the references in the fourth column. The

absolute abundances in each pulse are estimated using a calibrated OCS sample and have a margin of error of about an order of magnitude owing to uncertainties in the rotational temperature and instrument response function.

Molecule	Rotational transition	Frequency (MHz)	Reference	Absolute abundance (molecules/pulse)	Relative abundance
1,2,3-Trioxolane (POZ)	1 <sub>1,1</sub> -0 <sub>0,0</sub>	12,591.52	(29)	Not observed	—
O <sub>3</sub> + C <sub>2</sub> H <sub>4</sub> (1)	2 <sub>1,1</sub> -1 <sub>0,1</sub>	15,800.7834	(30)	3 × 10 <sup>12</sup>	500
CH <sub>2</sub> OO (2)	1 <sub>0,1</sub> -0 <sub>0,0</sub>	23,186.4873	(16, 17)	6 × 10 <sup>9</sup>	1
Formaldehyde* (3)	2 <sub>1,2</sub> -2 <sub>1,1</sub>	14,488.4803	(31)	2 × 10 <sup>16</sup>	3.3 × 10 <sup>6</sup>
Dioxirane (4)	2 <sub>1,1</sub> -2 <sub>0,2</sub>	31,752.8794	(32)	3 × 10 <sup>11</sup>	50
Formic acid (6)	1 <sub>0,1</sub> -0 <sub>0,0</sub>	22,471.1795	(33)	2 × 10 <sup>13</sup>	3333
Ethylene ozonide (8)	1 <sub>1,1</sub> -0 <sub>0,0</sub>	12,828.6233	(34)	5 × 10 <sup>11</sup>	83
Ethylene oxide (11)	1 <sub>1,0</sub> -1 <sub>0,1</sub>	11,385.9111	(35)	8 × 10 <sup>11</sup>	133
Acetaldehyde (12)	1 <sub>1,1</sub> -2 <sub>0,2</sub>	8,243.4683	(36)	7 × 10 <sup>12</sup>	1166
Formic anhydride (13)	2 <sub>1,2</sub> -1 <sub>1,1</sub>	11,734.1252	(37)	2 × 10 <sup>12</sup>	333

\*The only accessible transition of formaldehyde in the 5 to 42 GHz range of our spectrometer is a low-frequency *K*-type doublet, which makes the molecular abundance calculation less certain.

Our experimental results are in good agreement with this mechanism, as evidenced by the detection of ethylene ozonide, but in trace amounts relative to formic acid. Because the rotational spectrum of hydroxymethyl formate is unknown, its abundance could not be determined. Taatjes and co-workers (22) measured the reaction rate of CH<sub>2</sub>OO with acetaldehyde and found no evidence of secondary ozonide, but their experiments were done under low-pressure (4 torr) conditions, and secondary ozonide stabilization is likely pressure-dependent. The rate coefficient was recently estimated as  $k_A = 6.0 \times 10^{-13} \text{ cm}^3 \text{ molecule}^{-1} \text{ s}^{-1}$  (22, 43), but older studies (42) have reported values between  $10^{-12}$  and  $10^{-17} \text{ cm}^3 \text{ molecule}^{-1} \text{ s}^{-1}$ .

The reaction of CH<sub>2</sub>OO with C<sub>2</sub>H<sub>4</sub> (reaction B) was studied both experimentally (21) and theoretically (43, 44) and found to yield 1,2-dioxolane (10) through a barrierless pathway, although Crehuet *et al.* (44) suggest that a minor pathway, leading to ethylene oxide (11) and formaldehyde, is also possible. A portion of the ethylene oxide may isomerize to the more stable acetaldehyde isomer (12). We detected both 11 and 12, but the microwave spectrum of 10 has yet to be measured. Vereecken *et al.* (43) suggest an overall rate coefficient of  $k_B = 5.45 \times 10^{-15} \text{ cm}^3 \text{ molecule}^{-1} \text{ s}^{-1}$  for this reaction, but the experimental work of Buras *et al.* (21) indicates a rate coefficient of  $k_B = 7 \times 10^{-16} \text{ cm}^3 \text{ molecule}^{-1} \text{ s}^{-1}$ , nearly an order of magnitude smaller.

The reactions of CH<sub>2</sub>OO with ozone (reaction C) and with itself (reaction D) both yield formaldehyde and molecular oxygen. The former reacts with a rate coefficient of  $k_C = 1 \times 10^{-12} \text{ cm}^3 \text{ molecule}^{-1} \text{ s}^{-1}$  (43), although there is some disagreement about whether the reaction proceeds through a biradical (43) or a cyclic (45, 46) intermediate. Neither intermediate would likely be sufficiently stable for detection in our system, nor are there microwave spectral data available to test that hypothesis. Vereecken *et al.* (43) report that the CH<sub>2</sub>OO self-reaction proceeds exothermically through a cyclic biperioxide before decomposing to 2 CH<sub>2</sub>O + O<sub>2</sub>.

Buras and co-workers (47) have measured this rate coefficient as  $k_D = 6.0 \times 10^{-11} \text{ cm}^3 \text{ molecule}^{-1} \text{ s}^{-1}$ . Finally, CH<sub>2</sub>OO may react with CO to make formic anhydride (reaction E), as suggested by Kühne *et al.*

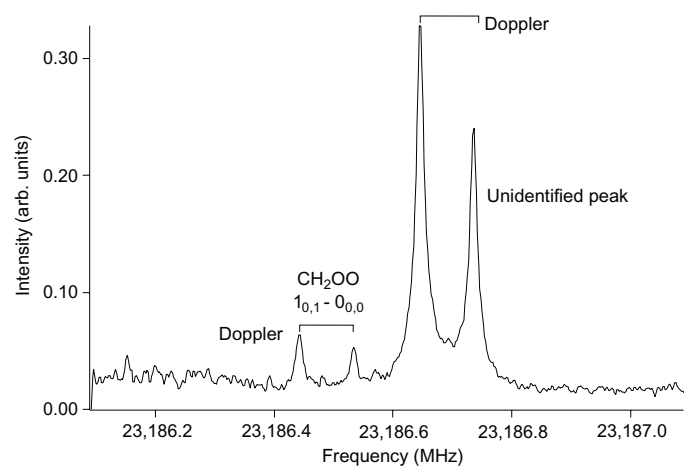


**Fig. 3. The fundamental rotational line (1<sub>0,1</sub>-0<sub>0,0</sub>) of the simplest CI, CH<sub>2</sub>OO, detected in the O<sub>3</sub> + C<sub>2</sub>H<sub>4</sub> reaction, acquired after 4.3 hours of integration, or 93,000 sample injections.** The peak is split into two Doppler components, a result of the alignment of the molecular beam with the two traveling waves of the Fabry-Pérot cavity. A more intense peak is visible, about 200 kHz higher in energy, the carrier of which remains unidentified.

(48). As CO is a dissociation product of vibrationally excited formic acid, this reaction is certainly possible, and we see evidence of formic anhydride (13). However, no experimental or theoretical rate constants have been published for this reaction, and we cannot measure the concentration of CO; thus, the importance of this reaction in our experiments remains unclear. Formic anhydride has also been suggested to be a product of the reaction of CH<sub>2</sub>OO with formic acid (49).

A simple kinetic model of the experimental CH<sub>2</sub>OO abundance is in qualitative agreement with the theoretically published rate constants. In this model, [CH<sub>2</sub>OO] was treated as a steady-state concentration, with its formation resulting from O<sub>3</sub> + C<sub>2</sub>H<sub>4</sub> alone [ $k_{\text{form}} = 1.45 \times 10^{-18} \text{ cm}^3 \text{ molecule}^{-1} \text{ s}^{-1}$  (10)], and its destruction occurring

through unimolecular reaction [ $k_{\text{uni}} = 75 \text{ s}^{-1}$  (22, 47)], and the bimolecular reactions listed in Fig. 5 involving species with large abundances ( $k_A$  through  $k_D$ ) only.

$$\frac{d[\text{CH}_2\text{OO}]}{dt} = k_{\text{form}}[\text{O}_3][\text{C}_2\text{H}_4] - k_{\text{uni}}[\text{CH}_2\text{OO}] - k_A[\text{CH}_2\text{OO}][\text{CH}_2\text{O}] - k_B[\text{CH}_2\text{OO}][\text{C}_2\text{H}_4] - k_C[\text{CH}_2\text{OO}][\text{O}_3] - k_D[\text{CH}_2\text{OO}]^2 \approx 0 \quad (1)$$

The concentrations of  $\text{O}_3$ ,  $\text{C}_2\text{H}_4$ , and  $\text{CH}_2\text{O}$  are large and were thus treated as constant. Equation 1 was solved for  $[\text{CH}_2\text{OO}]$  using the initial concentrations of  $[\text{O}_3] = 0.005 \text{ M}$  and  $[\text{C}_2\text{H}_4] = 0.0003 \text{ M}$ , and the experimentally measured  $[\text{CH}_2\text{O}] \lesssim 0.002 \text{ M}$ . Although several wide-ranging values of  $k_A$  and  $k_B$  have been published, neither has a large effect on  $[\text{CH}_2\text{OO}]$ , and thus, the most recently published value was selected. Other bimolecular reactions, including reaction E, were not included in this model because their rate coefficients have not been measured. The margins of error of all rate constants were assumed to be no smaller than an order of magnitude. This zeroth-order model, while rudimentary, predicts  $(3 \pm 1) \times 10^9 \text{ CH}_2\text{OO}$  molecules/pulse, in very good agreement with the about  $6 \times 10^9 \text{ molecules/pulse}$  detected. The estimated  $\text{CH}_2\text{O}$  abundance is uncertain because the only observable transition in the range of our spectrometer is a low-

frequency  $K$ -type doublet, and consequently, its value has been derived solely on the basis of a population difference between two closely spaced  $K$  levels rather than two rotational levels. The derived value is therefore larger than expected given the initial concentration of  $\text{C}_2\text{H}_4$ , but it is likely due to the organic mixture rich in formaldehyde that builds up over time inside the nozzle body (see Materials and Methods). Regardless, it should be emphasized that the results of the kinetic model are largely insensitive to the  $\text{CH}_2\text{O}$  concentration; an order of magnitude decrease in  $[\text{CH}_2\text{O}]$  results in a predicted steady-state value of  $[\text{CH}_2\text{OO}] = 3.7 \times 10^9 \text{ molecules/pulse}$ , which is well within the margin of error. We find instead that the reaction with ozone is the dominant destruction mechanism for  $\text{CH}_2\text{OO}$  in our model.

As demonstrated by the numerous observed species, the mechanism of the ozonolysis of ethylene is quite complex. Although the experimental results agree qualitatively with the simple kinetic model, an as-of-yet undiscovered mechanism may conceivably be responsible for some fraction of the steady-state  $\text{CH}_2\text{OO}$  abundance. For example, Wang *et al.* (50) calculated the energetic barriers and rate constants for the  $\text{CH}_2\text{O} + \text{O}_3$  reaction, and found  $\text{CH}_2\text{OO} + \text{O}_2$  to be a possible product channel. However, the barrier is higher than 60 kcal/mol, and the rate coefficient at 298 K was found to be on the order of  $10^{-33} \text{ cm}^3 \text{ molecule}^{-1} \text{ s}^{-1}$ . Given the concentration of ozone and formaldehyde found in these experiments, we would expect the formation of only  $10^2 \text{ CH}_2\text{OO}$  molecules/pulse from this mechanism. Similarly, the  $\text{CH}_2\text{OO}$  signal in our previous discharge studies of  $\text{CH}_4/\text{O}_2$  (16) was tentatively attributed to a secondary reaction of excited  $\text{CH}_3\text{OO}$  (51). However, only trace amounts of  $\text{CH}_3\text{OO}$  were detected in the present discharge-free experiments, and thus, this reaction is not expected to significantly contribute to the  $\text{CH}_2\text{OO}$  signal.

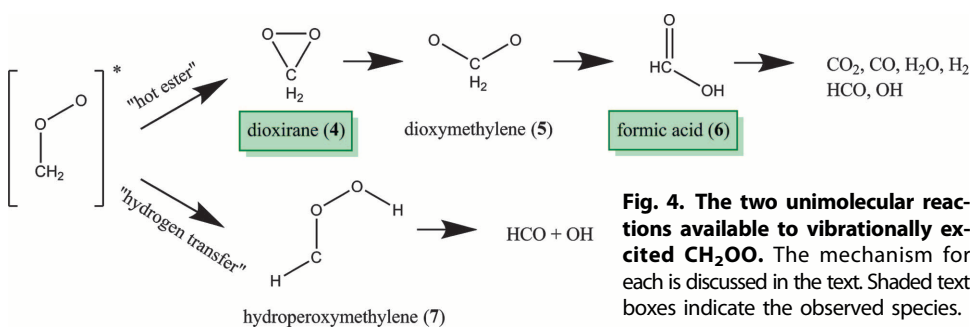


**Fig. 4. The two unimolecular reactions available to vibrationally excited  $\text{CH}_2\text{OO}$ .** The mechanism for each is discussed in the text. Shaded text boxes indicate the observed species.

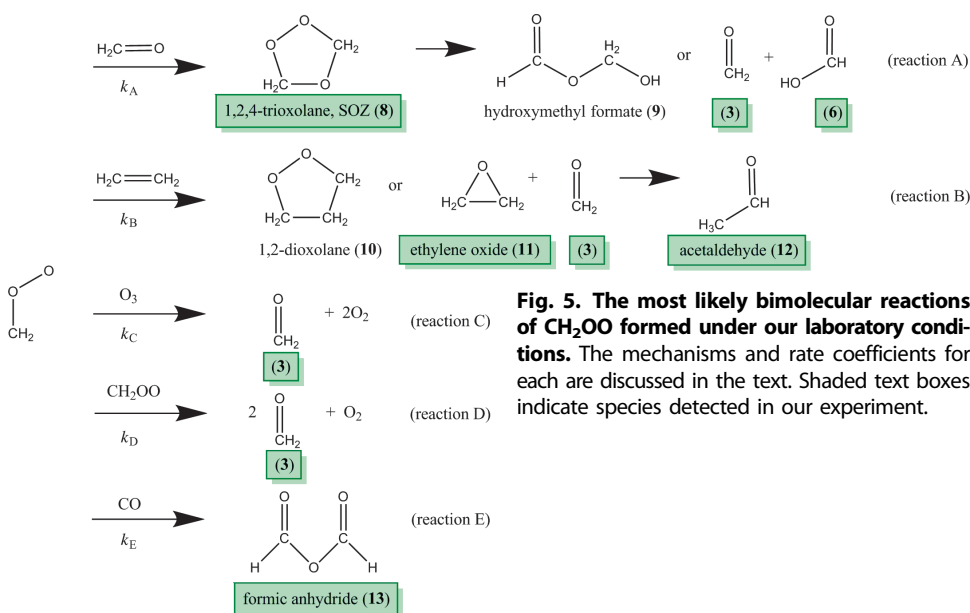


**Fig. 5. The most likely bimolecular reactions of  $\text{CH}_2\text{OO}$  formed under our laboratory conditions.** The mechanisms and rate coefficients for each are discussed in the text. Shaded text boxes indicate species detected in our experiment.

Experiments are currently under way to detect the monosubstituted CI,  $\text{CH}_3\text{CHOO}$ , via the reaction of  $\text{O}_3$  with  $\text{C}_3\text{H}_6$ . Under similar experimental conditions, many of the analogs to the products in the  $\text{O}_3 + \text{C}_2\text{H}_4$  reaction have been observed, including propylene ozonide, propylene oxide, *syn*-vinyl alcohol, propionaldehyde, acetic acid, and acetone, in addition to the formaldehyde, acetaldehyde, and formic acid found in the ethylene reaction. However, neither the  $\text{O}_3 \cdots \text{C}_3\text{H}_6$  van der Waals complex nor methyldioxirane,  $c\text{-(OOCH)-CH}_3$ , has been studied in the microwave region. Because detection of  $\text{O}_3 \cdots \text{C}_2\text{H}_4$  (1) and dioxirane (4) was a critical step in optimizing the experimental conditions in this study, our inability to optimize the experimental conditions in the  $\text{O}_3 + \text{C}_3\text{H}_6$  system using these analogs has made it difficult to definitively assign any signal to  $\text{CH}_3\text{CHOO}$ .

## CONCLUSIONS

We have reported the first detection of CH<sub>2</sub>OO in the gas-phase ozonolysis of ethylene at atmospheric temperature and pressure, using FTMW spectroscopy and a modified nozzle designed for rapid sampling. Although the signal was weak, it can be unequivocally attributed to CH<sub>2</sub>OO. Other products were detected in relative amounts that qualitatively support the established reaction pathways of the nascent excited and stabilized CIs in the literature. Although it is conceivable that an alternative mechanism is responsible for the CH<sub>2</sub>OO signal, the detected signals match very well with the kinetic model, and no other plausible mechanism has been suggested in the literature. Our results appear to confirm this long postulated oxidation mechanism. With improvements to the experimental methods described here, including developing a more consistent ozone source and increasing the steady-state concentration of CH<sub>2</sub>OO, this direct ozonolysis method may allow for the formation and characterization of larger CIs under atmospheric conditions. Direct formation from O<sub>3</sub> + alkenes greatly simplifies the formation kinetic analysis and can yield important information about branching and OH radical formation, which are key questions for understanding the critical role of ozonolysis in atmospheric chemistry.

## MATERIALS AND METHODS

In our nozzle design, two 1/16-inch-diameter holes were drilled into the inner body of a Parker-Hannifin Series 9 pulsed nozzle in a V-shape (Fig. 2). Stainless steel tubing (inner diameter 1/16 inch) was welded to each inlet, and O<sub>3</sub> and ethylene were separately passed into the nozzle, using mass flow controllers to regulate carefully their flow. In one inlet, 2% C<sub>2</sub>H<sub>4</sub> in neon flows at a rate of 50 sccm (cm<sup>3</sup>/min at STP), whereas a ~10% mixture of O<sub>3</sub> in argon flows through the second inlet at 100 sccm. The O<sub>3</sub> is obtained by trapping the ozone from a Welsbach ozonator on a silica gel trap maintained at -60°C and then flowing argon through the trap. Ozone is explosive in high concentrations, so for safety we collected very small samples of ozone on the trap (<500 mg) and refilled it every 2 hours. The rate of desorption of O<sub>3</sub> is roughly proportional to the trapped concentration; thus, a high initial ozone concentration is observed (quantified by sodium thiosulfate titration), followed by a steady decrease over 2 hours. The concentration of O<sub>3</sub> inside the nozzle can therefore only be estimated.

The reactants mix at 1 atm and 298 K inside the 1.6-cm<sup>3</sup> body of the nozzle, and the pulsed nozzle injects ~3.5% of the resulting mixture into the FTMW spectrometer; the remainder of the gas vents through the rear of the nozzle. We estimate that the products are sampled within the first 0.5 s of the reaction because there is a high steady gas flow and sampling occurs at a rate of 6 Hz. The signal levels began to diminish after about 2 hours, ostensibly owing to the buildup of a thin film of organic material on the inside of the nozzle, which required manual cleaning. The microwave spectrum obtained by flowing an inert gas over this material indicates the presence of formic acid and formaldehyde, but the low volatility of the material suggests the additional presence of larger oligomers.

A portion of the reaction mixture is supersonically expanded ( $T_{\text{rot}} \approx 3$  K) into a vacuum chamber maintained at 10<sup>-6</sup> torr, and probed by a 5 to 42 GHz cavity FTMW spectrometer. A tunable microwave synthesizer generates ~1 μs microwave pulses, which excites all rotational trans-

sitions that fall within the bandwidth of the pulse. Coherently rotating molecules undergo free induction decay, which is detected using a sensitive microwave receiver; a Fourier transform of this signal yields a power spectrum. Products in the O<sub>3</sub> + C<sub>2</sub>H<sub>4</sub> reaction are detected by monitoring known low-*J* rotational transitions of each. No attempt was made to detect species whose microwave transitions have yet to be measured. The species detected are shown in Table 1, along with their molecular abundances, estimated by calibrating with a stable molecule of known abundance [0.04% carbonyl sulfide (OCS) in Ar] and corrected for differences in dipole moments, rotational partition functions, and the spectrometer instrument response function.

## REFERENCES

1. D. Johnson, G. Marston, The gas-phase ozonolysis of unsaturated volatile organic compounds in the troposphere. *Chem. Soc. Rev.* **37**, 699–716 (2008).
2. C. A. Taatjes, D. E. Shallcross, C. J. Percival, Research frontiers in the chemistry of Criegee intermediates and tropospheric ozonolysis. *Phys. Chem. Chem. Phys.* **16**, 1704–1718 (2014).
3. N. M. Donahue, G. T. Drozd, S. A. Epstein, A. A. Presto, J. H. Kroll, Adventures in ozoneland: Down the rabbit-hole. *Phys. Chem. Chem. Phys.* **13**, 10848–10857 (2011).
4. L. Vereecken, J. S. Francisco, Theoretical studies of atmospheric reaction mechanisms in the troposphere. *Chem. Soc. Rev.* **41**, 6259–6293 (2012).
5. M. Olzmann, E. Kraka, D. Cremer, R. Gutbrod, S. Andersson, Energetics, kinetics, and product distributions of the reactions of ozone with ethene and 2,3-dimethyl-2-butene. *J. Phys. Chem. A* **101**, 9421–9429 (1997).
6. J. Li, S. Carter, J. M. Bowman, R. Dawes, D. Xie, H. Guo, High-level, first-principles, full-dimensional quantum calculation of the rovibrational spectrum of the simplest Criegee intermediate (CH<sub>2</sub>OO). *J. Phys. Chem. Lett.* **5**, 2364–2369 (2014).
7. Y.-T. Su, H.-Y. Lin, R. Putikam, H. Matsui, M. C. Lin, Y.-P. Lee, Extremely rapid self-reaction of the simplest Criegee intermediate CH<sub>2</sub>OO and its implications in atmospheric chemistry. *Nat. Chem.* **6**, 477–483 (2014).
8. J. Ahrens, P. T. M. Carlsson, N. Hertl, M. Olzmann, M. Pfeifle, J. L. Wolf, T. Zeuch, Infrared detection of Criegee intermediates formed during the ozonolysis of β-pinene and their reactivity towards sulfur dioxide. *Angew. Chem. Int. Ed. Engl.* **53**, 715–719 (2014).
9. R. Atkinson, Gas-phase tropospheric chemistry of volatile organic compounds: 1. Alkanes and alkenes. *J. Phys. Chem. Ref. Data* **26**, 215–290 (1997).
10. M. S. Alam, M. Camredon, A. R. Rickard, T. Carr, K. P. Wyche, K. E. Hornsby, P. S. Monks, W. J. Bloss, Total radical yields from tropospheric ethene ozonolysis. *Phys. Chem. Chem. Phys.* **13**, 11002–11015 (2011).
11. G. T. Drozd, N. M. Donahue, Pressure dependence of stabilized Criegee intermediate formation from a sequence of alkenes. *J. Phys. Chem. A* **115**, 4381–4387 (2011).
12. C. Geletneký, S. Berger, The mechanism of ozonolysis revisited by <sup>17</sup>O-NMR spectroscopy. *Eur. J. Org. Chem.* **1998**, 1625–1627 (1998).
13. C. A. Taatjes, G. Meloni, T. M. Selby, A. J. Trevitt, D. L. Osborn, C. J. Percival, D. E. Shallcross, Direct observation of the gas-phase Criegee intermediate (CH<sub>2</sub>OO). *J. Am. Chem. Soc.* **130**, 11883–11885 (2008).
14. O. Welz, J. D. Savee, D. L. Osborn, S. S. Vasu, C. J. Percival, D. E. Shallcross, C. A. Taatjes, Direct kinetic measurements of Criegee intermediate (CH<sub>2</sub>OO) formed by reaction of CH<sub>2</sub> with O<sub>2</sub>. *Science* **335**, 204–207 (2012).
15. Y.-T. Su, Y.-H. Huang, H. A. Witek, Y.-P. Lee, Infrared absorption spectrum of the simplest Criegee intermediate CH<sub>2</sub>OO. *Science* **340**, 174–176 (2013).
16. M. C. McCarthy, L. Cheng, K. N. Crabtree, O. Martinez Jr., T. L. Nguyen, C. C. Womack, J. F. Stanton, The simplest Criegee intermediate (H<sub>2</sub>COO): Isotopic spectroscopy, equilibrium structure, and possible formation from atmospheric lightning. *J. Phys. Chem. Lett.* **4**, 4133–4139 (2013).
17. M. Nakajima, Y. Endo, Determination of the molecular structure of the simplest Criegee intermediate CH<sub>2</sub>OO. *J. Chem. Phys.* **139**, 101103 (2013).
18. M. Nakajima, Y. Endo, Spectroscopic characterization of an alkyl substituted Criegee intermediate *syn*-CH<sub>3</sub>CHOO through pure rotational transitions. *J. Chem. Phys.* **140**, 011101 (2014).
19. J. M. Beames, F. Liu, L. Lu, M. I. Lester, Ultraviolet spectrum and photochemistry of the simplest Criegee intermediate CH<sub>2</sub>OO. *J. Am. Chem. Soc.* **134**, 20045–20048 (2012).
20. J. H. Lehman, H. Li, J. M. Beames, M. I. Lester, Ultraviolet photodissociation dynamics of the simplest Criegee intermediate CH<sub>2</sub>OO. *J. Chem. Phys.* **139**, 141103 (2013).

21. Z. J. Buras, R. M. I. Elsamra, A. Jalan, J. E. Middaugh, W. H. Green, Direct kinetic measurements of reactions between the simplest Criegee intermediate  $\text{CH}_2\text{OO}$  and alkenes. *J. Phys. Chem. A* **118**, 1997–2006 (2014).
22. C. A. Taatjes, O. Welz, A. J. Eskola, J. D. Savee, D. L. Osborn, E. P. Lee, J. M. Dyke, D. W. Mok, D. E. Shallcross, C. J. Percival, Direct measurement of Criegee intermediate ( $\text{CH}_2\text{OO}$ ) reactions with acetone, acetaldehyde, and hexafluoroacetone. *Phys. Chem. Chem. Phys.* **14**, 10391–10400 (2012).
23. C. A. Taatjes, O. Welz, A. J. Eskola, J. D. Savee, A. M. Scheer, D. E. Shallcross, B. Rotavera, E. P. Lee, J. M. Dyke, D. K. Mok, D. L. Osborn, C. J. Percival, Direct measurements of conformer-dependent reactivity of the Criegee intermediate  $\text{CH}_3\text{CHOO}$ . *Science* **340**, 177–180 (2013).
24. J. M. Anglada, R. Crehuet, J. M. Bofill, The ozonolysis of ethylene: A theoretical study of the gas-phase reaction mechanism. *Chem. Eur. J.* **5**, 1809–1822 (1999).
25. R. Ponec, J. Roithová, Y. Haas, Mechanism of gas phase ethene-ozone reaction and concomitant processes. Theoretical study. *Croat. Chem. Acta* **74**, 251–264 (2001).
26. T. J. Balle, W. H. Flygare, Fabry-Pérot cavity pulsed Fourier transform microwave spectrometer with a pulsed nozzle particle source. *Rev. Sci. Instrum.* **52**, 33–45 (1981).
27. C. W. Gillies, J. Z. Gillies, R. D. Suenram, F. J. Lovas, E. Kraka, D. Cremer, Van der Waals complexes in 1,3-dipolar cycloaddition reactions: Ozone-ethylene. *J. Am. Chem. Soc.* **113**, 2412–2421 (1991).
28. J. Z. Gillies, C. W. Gillies, F. J. Lovas, K. Matsumura, R. D. Suenram, E. Kraka, D. Cremer, Van der Waals complexes of chemically reactive gases: Ozone-acetylene. *J. Am. Chem. Soc.* **113**, 6408–6415 (1991).
29. J. Zozom, C. W. Gillies, R. D. Suenram, F. J. Lovas, Microwave detection of the primary ozonide of ethylene in the gas phase. *Chem. Phys. Lett.* **140**, 64–70 (1987).
30. J. Z. Gillies, C. W. Gillies, R. D. Suenram, F. J. Lovas, W. Stahl, The microwave spectrum and molecular structure of the ethylene-ozone van der Waals complex. *J. Am. Chem. Soc.* **111**, 3073–3074 (1989).
31. R. Bocquet, J. Demaison, L. Poteau, M. Liedtke, S. Belov, K. M. T. Yamada, G. Winnewisser, C. Gerke, J. Gripp, T. Köhler, The ground state rotational spectrum of formaldehyde. *J. Mol. Spectrosc.* **177**, 154–159 (1996).
32. R. D. Suenram, F. J. Lovas, Dioxirane. Its synthesis, microwave spectrum, structure, and dipole moment. *J. Am. Chem. Soc.* **100**, 5117–5122 (1978).
33. M. Winnewisser, B. P. Winnewisser, M. Stein, M. Birk, G. Wagner, G. Winnewisser, K. M. T. Yamada, S. P. Belov, O. I. Baskakov, Rotational spectra of *cis*-HCOOH, *trans*-HCOOH, and *trans*-H<sup>13</sup>COOH. *J. Mol. Spectrosc.* **216**, 259–265 (2002).
34. C. W. Gillies, R. L. Kuczkowski, Mechanism of ozonolysis. Microwave spectrum, structure, and dipole moment of ethylene ozonide. *J. Am. Chem. Soc.* **94**, 6337–6343 (1972).
35. J. Pan, A. Sieghard, K. V. L. N. Sastry, E. Herbst, F. C. De Lucia, The millimeter- and sub-millimeter-wave spectrum of ethylene oxide (*c*- $\text{C}_2\text{H}_4\text{O}$ ). *Astrophys. J.* **499**, 517–519 (1998).
36. I. Kleiner, F. J. Lovas, M. Godefroid, Microwave spectra of molecules of astrophysical interest. XXIII. Acetaldehyde. *J. Phys. Chem. Ref. Data* **25**, 1113–1210 (1996).
37. S. Vaccani, A. Bauder, Hs. H. Günthard, Microwave spectrum, dipole moment and conformation of formic anhydride. *Chem. Phys. Lett.* **35**, 457–460 (1975).
38. J. H. Kroll, N. M. Donahue, V. J. Cee, K. L. Demerjian, J. G. Anderson, Gas-phase ozonolysis of alkenes: Formation of OH from anti carbonyl oxides. *J. Am. Chem. Soc.* **124**, 8518–8519 (2002).
39. R. Gutbrod, R. N. Schindler, E. Kraka, D. Cremer, Formation of OH radicals in the gas phase ozonolysis of alkenes: The unexpected role of carbonyl oxides. *Chem. Phys. Lett.* **252**, 221–229 (1996).
40. J. M. Anglada, J. González, M. Torrent-Sucarrat, Effects of the substituents on the reactivity of carbonyl oxides. A theoretical study on the reaction of substituted carbonyl oxides with water. *Phys. Chem. Chem. Phys.* **13**, 13034–13045 (2011).
41. L. Vereecken, H. Harder, A. Novelli, The reaction of Criegee intermediates with NO,  $\text{RO}_2$ , and  $\text{SO}_2$ , and their fate in the atmosphere. *Phys. Chem. Chem. Phys.* **14**, 14682–14695 (2012).
42. J. D. Fenske, A. S. Hasson, A. W. Ho, S. E. Paulson, Measurement of absolute unimolecular and bimolecular rate constants for  $\text{CH}_3\text{CHOO}$  generated by the *trans*-2-butene reaction with ozone in the gas phase. *J. Phys. Chem. A* **104**, 9921–9932 (2000).
43. L. Vereecken, H. Harder, A. Novelli, The reactions of Criegee intermediates with alkenes, ozone, and carbonyl oxides. *Phys. Chem. Chem. Phys.* **16**, 4039–4049 (2014).
44. R. Crehuet, J. M. Anglada, D. Cremer, J. M. Bofill, Reaction modes of carbonyl oxide, dioxirane, and methylenebis(oxy) with ethylene: A new reaction mechanism. *J. Phys. Chem. A* **106**, 3917–3929 (2002).
45. H. G. Kjaergaard, T. Kurtén, L. B. Nielsen, S. Jørgensen, P. O. Wennberg, Criegee intermediates react with ozone. *J. Phys. Chem. Lett.* **4**, 2525–2529 (2013).
46. W. M. Wei, R. H. Zheng, Y. L. Pan, Y. K. Wu, F. Yang, S. Hong, Ozone dissociation to oxygen affected by Criegee intermediate. *J. Phys. Chem. A* **118**, 1644–1650 (2014).
47. Z. J. Buras, R. M. I. Elsamra, W. H. Green, Direct determination of the simplest Criegee intermediate ( $\text{CH}_2\text{OO}$ ) self reaction rate. *J. Phys. Chem. Lett.* **5**, 2224–2228 (2014).
48. H. Kühne, S. Vaccani, T. K. Ha, A. Bauder, H. H. Günthard, Infrared-matrix and microwave spectroscopy of the ethylene-ozone gas-phase reaction. *Chem. Phys. Lett.* **38**, 449–455 (1976).
49. H. Osada, Y. Morikawa, T. Nishiwaki, S. Sekiya, Proof of the formation of hydroperoxymethyl formate in the ozonolysis of ethene: Synthesis and FT-IR spectra of the authentic compound. *Chem. Phys. Lett.* **258**, 155–158 (1996).
50. F. Wang, H. Sun, J. Sun, X. Jia, Y. Zhang, Y. Tang, X. Pan, Z. Su, L. Hao, R. Wang, Mechanistic and kinetic study of  $\text{CH}_2\text{O}+\text{O}_3$  reaction. *J. Phys. Chem. A* **114**, 3516–3522 (2010).
51. T. L. Nguyen, M. C. McCarthy, J. F. Stanton, Relatively selective production of the simplest Criegee intermediate in a  $\text{CH}_4/\text{O}_2$  electric discharge: Kinetic analysis of a plausible mechanism. *J. Phys. Chem. A* (2014).

**Acknowledgments:** We gratefully acknowledge F. Lovas, J. Stanton, T. Lam Nguyen, W. Green, Z. Buras, and J. Kroll for helpful discussions. We would also like to thank W. Pringle for the loan of an ozonator, E. S. Palmer and P. Antonucci for technical assistance, and K. Crabtree for developing the data acquisition software. **Funding:** This work was supported by the National Science Foundation under grant no. CHE-1058063. C.C.W. acknowledges the support of the Camille and Henry Dreyfus Foundation Postdoctoral Program in Environmental Chemistry. **Author contributions:** C.C.W., M.-A.M.-D., and G.G.B. collected the data; C.C.W., R.W.F., and M.C.M. designed the study; and C.C.W. and M.C.M. wrote the manuscript. **Competing interests:** The authors declare that they have no competing financial interests.

Submitted 14 November 2014

Accepted 6 February 2015

Published 6 March 2015

10.1126/sciadv.1400105

**Citation:** C. C. Womack, M.-A. Martin-Drumel, G. G. Brown, R. W. Field, M. C. McCarthy, Observation of the simplest Criegee intermediate  $\text{CH}_2\text{OO}$  in the gas-phase ozonolysis of ethylene. *Sci. Adv.* **1**, e1400105 (2015).

## Observation of the simplest Criegee intermediate CH<sub>2</sub>OO in the gas-phase ozonolysis of ethylene

Caroline C. Womack, Marie-Aline Martin-Drumel, Gordon G. Brown, Robert W. Field and Michael C. McCarthy

*Sci Adv* 1 (2), e1400105.  
DOI: 10.1126/sciadv.1400105

**ARTICLE TOOLS** <http://advances.sciencemag.org/content/1/2/e1400105>

**REFERENCES** This article cites 50 articles, 3 of which you can access for free  
<http://advances.sciencemag.org/content/1/2/e1400105#BIBL>

**PERMISSIONS** <http://www.sciencemag.org/help/reprints-and-permissions>

Use of this article is subject to the [Terms of Service](#)

---

*Science Advances* (ISSN 2375-2548) is published by the American Association for the Advancement of Science, 1200 New York Avenue NW, Washington, DC 20005. The title *Science Advances* is a registered trademark of AAAS.

Copyright © 2015, The Authors